[26]C. J. Hwang, J. Appl. Phys. 39, 4307 (1968).
[27]B. L. Gregory, J. Appl. Phys. 36, 3765 (1965).
[28]L. W. Aukerman, M. F. Millea, and M. McColl, J. Appl. Phys. 38, 685 (1967).
[29]T. S. Rao-Sahib and D. B. Wittry, J. Appl. Phys. 40, 3745 (1969).
[30]C. E. Barnes, IEEE Trans. Nucl. Sci. NS-16, 28 (1969).
[31]B. L. Gregory and C. E. Barnes (unpublished).
[32]H. Nelson, J. I. Pankove, F. Hawrylo, G. C. Dousmanis, and C. Reno, Proc. IEEE 52, 1360 (1964).
[33]J. W. Corbett, *Electron Radiation Damage in Semiconductors and Metals* (Academic, New York, 1966).
[34]F. L. Vook, Phys. Rev. 135, A1742 (1964).
[35]F. L. Vook, Appl. Phys. Letters 13, 25 (1968).
[36]H. J. Stein, J. Appl. Phys. 40, 5300 (1969).
[37]H. R. Potts and G. L. Pearson, J. Appl. Phys. 37, 2098 (1966).
[38]G. W. Gobeli and G. W. Arnold, Bull. Am. Phys. Soc. 10, 321 (1965).
[39]G. D. Watkins, J. Phys. Soc. Japan 18, 22 (1963).
[40]H. Kressel and N. E. Byer, IEEE Proc. 57, 25 (1969).
[41]C. Lanza, K. L. Konnerth, and C. E. Kelly, Solid-State Electron. 10, 21 (1967).
[42]W. N. Jacobus, Solid-State Electron. 10, 260 (1967).
[43]S. A. Steiner and R. L. Anderson, Solid-State Electron. 11, 65 (1968).

PHYSICAL REVIEW B VOLUME 1, NUMBER 12 15 JUNE 1970

Electronic Band Structure and Optical Properties of Graphite from a Variational Approach*

G. S. Painter
Metals and Ceramics Division, Oak Ridge National Laboratory, Oak Ridge, Tennessee 37830
and
D. E. Ellis†
Physics Department, Northwestern University, Evanston, Illinois 60201
(Received 26 January 1970)

The electronic band structure of graphite has been calculated from an *ab initio* variational approach using a linear-combination of atomic-orbitals (LCAO) basis of Bloch states, including nonspherical terms in the one-electron crystal potential. Matrix elements of the Hamiltonian are evaluated directly without any tight-binding approximations. The optical transitions deduced from the energy bands calculated using a single-layer crystal model agree nicely with recent polarized-light reflectance measurements. Details of the band structure are calculated for the three-dimensional Brillouin zone and related to the results obtained using the single-layer crystal structure. The results are encouraging, not only from the standpoint that the method employed is an *ab initio* approach with no special *a priori* assumptions, but also because the band structure is quite insensitive to the particulars of the crystal potential function.

I. INTRODUCTION

There has been much interest recently in the properties of crystals exhibiting strongly anisotropic behavior: Of these, graphite is an excellent example of a substance illustrating the effects of greatly differing bonding in different crystallographic directions. While the carbon atoms in the cleavage planes of graphite are strongly bound among themselves, the adjacent planes are bonded together very weakly.

As a consequence of the large interlayer spacing in graphite, most of the optical characteristics of the substance can be well understood on the basis of a single-layer crystal structure.[1] Reflection in the layer plane σ_h is a symmetry operation for the single layer, and states can be classified according to their parity with respect to σ_h. Thus selection rules can be easily determined for transitions with the incident electric field parallel or perpendicular to the c axis. Since the interaction between different planes is small, the breakdown of the selection rules in the three-dimensional Brillouin zone for $k_z \neq n\pi/c$ is such that transitions "forbidden" for the single-layer structure still are not expected to contribute very significantly for the multiple-layer crystal. Thus, optical experiments with polarized light can be quite useful in gaining an understanding of the electronic structure of graphite.

Experimental results on the anisotropy of the optical constants of graphite have recently been determined[1] in the energy range 2–10 eV. As far as the optical properties are concerned, it turns

out that the assumption that the interaction between layers is a small perturbation is justified, and the energy variation with k_z is small. However, for explaining the electrical properties of graphite, it is necessary to account for the interaction between π bands.[2-5]

While there exist numerous theoretical treatments of the electronic structure of graphite,[6-10] most band theoretical investigations have employed the tight-binding model, with the introduction of adjustable parameters in the solution of the problem. Although considerable success has been obtained from these semiempirical-type calculations in predicting certain features of the optical data,[1] some discrepancies still exist.

The purpose of this investigation was therefore twofold: first, to apply a completely *ab initio* type of variational approach to calculate the energy band structure in the one-electron model and to compare the results of this model with those from semiempirical solutions and, second, to relate the observed optical transitions to the calculated band structure.

II. METHOD

The direct variational approach to the energy band problem has been described previously.[11] Hence, only a brief description of the method will be presented here. In a Bloch basis $\{\chi_i(\vec{k};\vec{r})\}$ with a one-electron Hamiltonian (in hartree atomic units)

$$\mathcal{H}(\vec{r}) = -\tfrac{1}{2}\nabla^2 + V(\vec{r}) \quad . \tag{1}$$

Variational solutions

$$\psi_i(\vec{k},\vec{r}) = \Sigma_j \chi_j(\vec{k},\vec{r}) C_{ji}(\vec{k}) \tag{2}$$

are obtained from the secular matrix equation

$$\mathbf{H}(\vec{k})\mathbf{C}(\vec{k}) = \epsilon(\vec{k})\mathbf{S}(\vec{k})\mathbf{C}(\vec{k}) \ ,$$

$$H_{ij} = \langle \chi_i | \mathcal{H} | \chi_j \rangle \ , \quad S_{ij} = \langle \chi_i | \chi_j \rangle \ . \tag{3}$$

In this method, we employ a numerical integration over a single unit cell of all relevant matrix elements in setting up the secular equations:

$$H_{ij}(\vec{k}) = \sum_{m=1}^{M} w(\vec{r}_m)\chi_i^*(\vec{k},\vec{r}_m)\mathcal{H}(\vec{r}_m)\chi_j(\vec{k},\vec{r}_m) \tag{4}$$

with $w(\vec{r}_m)$ the integration weight function, and the points $\vec{r}_m$ confined to one cell.

The Bloch basis functions $\chi_i(\vec{k},\vec{r})$ are constructed from atomiclike basis functions

$$a_i(\vec{r}) = \chi^{l_i} y^{m_i} z^{n_i} r^{p_i} e^{-\beta_i r} \ , \tag{5}$$

$$\chi_i(\vec{k},\vec{r}) = \sum_\nu e^{i\vec{k}\cdot\vec{R}_\nu} a_i(\vec{r} - \vec{R}_\nu - \vec{\mu}_i) \ . \tag{6}$$

The lattice sum is over the repeating volume of N cells and $\vec{\mu}_i$ is a nonprimitive vector specifying an atom in the cell at lattice site $\vec{R}_\nu$. The atomic basis used to converge the graphite band structure is given in Table I.

TABLE I. Atomic basis functions for LCAO Bloch orbitals for graphite.

$1s$		$e^{-5.4r}$
$2s$	r	
$2px$	x	$e^{-1.4r}$
$2py$	y	
$2pz$	z	
$2s'$	r	
$2px'$	x	$e^{-2.8r}$
$2py'$	y	
$2pz'$	z	

The crystal potential is formed by a direct superposition of free-atom Coulomb potentials and charge densities at each integration point and forming the $\rho^{1/3}$ local approximation to the exchange potential

$$V(\vec{r}_m) = \sum_{\nu,\mu} V_a(\vec{r}_m - \vec{R}_\nu - \vec{\mu}) - 3\alpha\left(\tfrac{3}{8\pi}\sum_{\nu,\mu}\rho_a(\vec{r}_m - \vec{R}_\nu - \vec{\mu})\right)^{1/3} .$$

The constant α can be used to scale the crystal exchange potential. The free-carbon-atom Coulomb potential $V_a(r)$ and charge density $\rho_a(r)$ were generated from the Herman-Skillman program.[12]

Nonspherical contributions to $V(\vec{r}_m)$ are retained, and as they are quite non-negligible (~0.5 hartree peak-to-peak amplitude at the atomic radius of 1.3425 a.u.) a muffin-tin potential approximation would not be expected to yield meaningful results for graphite. While calculations were not carried to self-consistency, two exchange potentials were used, one with the full Slater exchange ($\alpha = 1.0$) and the other with the χ_α exchange[13] value of $\alpha = 0.76$. It is encouraging that the results obtained for these two values of α differed negligibly.

Calculations were initially performed for the single-layer structure for which the unit cell is the two-dimensional parallelogram described by the primitive vectors $\vec{t}_1 = \frac{1}{2}a(\sqrt{3}, -1, 0)$ and $\vec{t}_2 = a(0, 1, 0)$, where the lattice constant a was taken to be 2.46 Å. The two carbon atoms per unit cell occupy the positions (0, 0, 0) and $\frac{1}{2}a(1/\sqrt{3}, 1, 0)$ in the central unit cell.

In order to investigate the over-all effects on the band structure of the interaction between layers, and, in particular, to compute the splittings at certain points in the Brillouin zone, computations were carried out for the four atoms per unit cell structure illustrated in Fig. 1. The third primitive vector in this case is $\vec{t}_3 = (0, 0, c)$, where $c = 6.70$ Å. To facilitate the subsequent selection-rule analysis at symmetry points in the Brillouin

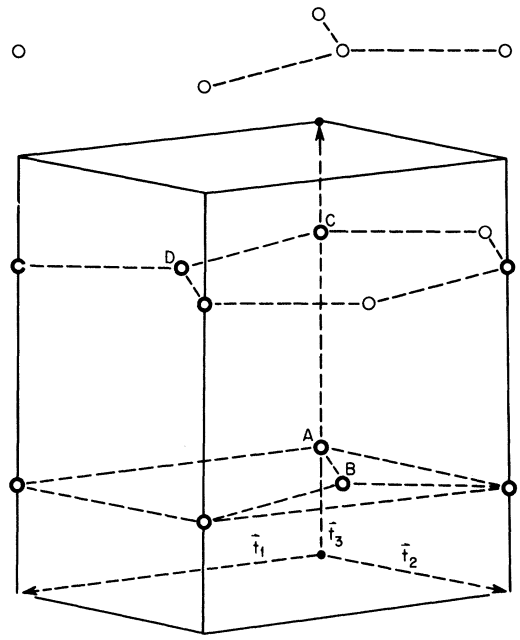

FIG. 1. Graphite crystal-lattice structure. The solid-line parallelopiped is the unit cell containing four atoms labeled *A*, *B*, *C*, *D* with the origin of the cell on the *BD* bond center. The heavy-lined circles denote atoms either inside or on the boundary of the central unit cell; the lighter circles denote atoms outside the central cell. The unit cell for the single-layer crystal is the parallelogram containing atoms *A* and *B* in the plane $z = -\frac{1}{4}c$. Primitive vector $\vec{t}_3$ lies along the *c* axis.

zone (illustrated for the three-dimensional case in Fig. 2) the origin of the parallelopiped was chosen to lie at the midpoint of the line joining atoms *B* and *D* (Fig. 1), which is a site of inversion symmetry. The carbon atoms then occupy positions

$$\vec{\mu}_A = \tfrac{1}{4}(-a\sqrt{3}, -a, -c), \quad \vec{\mu}_C = \tfrac{1}{4}(-a\sqrt{3}, -a, c),$$
$$\vec{\mu}_B = \tfrac{1}{4}(-a/\sqrt{3}, a, -c) = -\vec{\mu}_D .$$

Integration point distributions were generated at each of the four atom sites in the unit cell with appropriate translations back into the parallelopiped for points falling outside the central unit cell. The energy band structure (Fig. 3) was converged to within 0.005 hartree with 300 integration points per atom and a lattice sum over about 40 atoms. Actually, the occupied bands stabilize to greater accuracy (0.002 hartree) than the excited bands.

III. RESULTS

From a comparison of energies obtained by treating the single-layer structure (18 basis functions) and the four atom per unit cell case, including interactions with near-neighbor planes (36 basis functions), we find, in agreement with other works,[1,14,15] that the over-all features of the optical reflectance data are adequately described by the single-layer band structure. The energy band structure obtained in the multiple-layer crystal is not very dependent upon the wave vector k_z along the *z* axis of the three-dimensional Brillouin zone.

Hence, an examination of the bands in the two-dimensional Brillouin zone formed by the $k_z = 0$ plane of Fig. 2 elucidates the corresponding structure in planes k_z = constant of the actual three-dimensional Brillouin zone. In this case, the optical transitions determined from the two-dimensional band structure should be nearly the same as those which would result from an analysis of the three-dimensional Brillouin zone. For this reason and from the existing calculations[10] of the joint density of states from the energy bands, it is justified to make assignments of optical transitions to the bands of the single-layer model (Fig. 3). A more thorough analysis can be made by computing the joint density of states and the imaginary part of the dielectric function.

A. Relation of Band Structure to Optical Properties

In Fig. 3, we present the results of the calculation using the single-layer model. For this case, the Brillouin zone is the two-dimensional figure formed by the $k_z = 0$ plane of Fig. 2. The calculation of the single-layer band structure was done in about 80 sec on the IBM 360-91 at Oak Ridge National Laboratory. The valence bandwidth of Fig. 3 is about 19.3 eV, in good agreement with the soft x-ray emission spectral result (18 eV) of Chalklin.[16] The general features of the band structure of Fig. 3 are in qualitative agreement with existing recent calculations of Bassani and Pastori Parravicini.[10] However, there are important quantitative differences in the energies and the assignments of optical transitions.

In Fig. 3, we label the linear combinations of

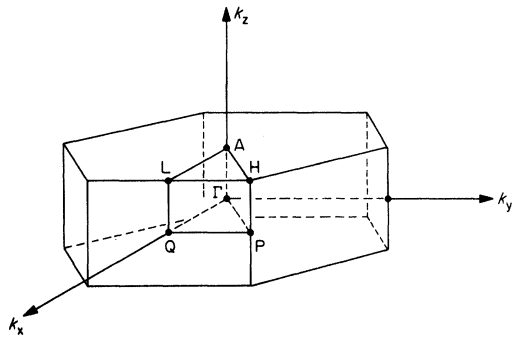

FIG. 2. Brillouin zone for graphite. For the single-layer crystal, the Brillouin zone is the hexagon formed by the intersection with the plane $k_z = 0$.

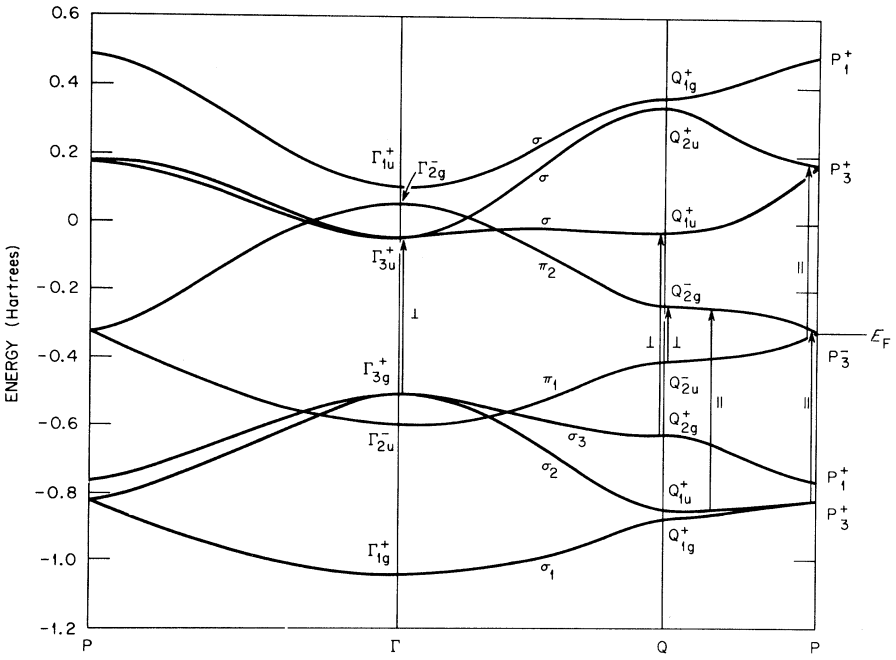

FIG. 3. Energy band structure for graphite in the single-layer crystal model. Allowed transitions which contribute structure to the reflectance are indicated for polarization parallel (∥) and perpendicular (⊥) to the c axis.

Bloch eigenfunctions by the irreducible representations they span, using the notation of Ref. 10 [superscripts + and − label representations even and odd under reflection $\{\sigma_h, 0\}$ in the layer, and subscripts g and u denote representations even and odd under the operation $\{I \mid \vec{f}\}$, inversion through the origin at (0, 0, 0) and translation by $\vec{f} = \frac{1}{3}\vec{t}_1 + \frac{2}{3}\vec{t}_2$]. One feature of the method used in this calculation is that the wave function, in terms of the linear combinations of Bloch states [Eq. (2)], is explicitly known and thus electric dipole transition probabilities, given by $M_{lm}(\vec{k}) \propto |\langle \psi_l(\vec{k}) | \vec{r} | \psi_m(\vec{k}) \rangle|^2$, can be directly calculated. Since the atomic basis set used in this calculation is expressed in powers of x, y, and z, we can use the characters of the irreducible representation to which $\vec{r}$ and these powers belong to derive selection rules.[17] Thus, the wave functions are symmetry classified in Fig. 3 and the allowed transitions for incident radiation polarized along the c axis $E \parallel c$ and perpendicular to this axis $E \perp c$ are indicated by vertical lines at high symmetry points in the Brillouin zone.

The results of the unpolarized near-normal reflectance measurements of Taft and Philipp[14] on natural graphite, and of Carter *et al.*[15] on pyrolytic graphite, demonstrate a narrow peak in the imaginary part of the dielectric constant at 4.5 eV and a broad peak at 14.5 eV. Greenaway *et al.*[1] observed a peak in reflectivity for polarization $E \perp c$ at about 4.6 eV, which they ascribe to Q^-_{2g}-Q^-_{2u} transitions. This is in good agreement with our calculation, which gives a separation of 4.6 eV between the π bands at the critical point Q. We consider the shoulder on this peak at about 6 eV, which Greenaway *et al.*[1] ascribe to zone-center transitions, to be a result of the structure in the π bands near Q. On the other hand, from the results of our calculation the Γ^+_{3g}-Γ^+_{3u} transition allowed for $E \perp c$ occurs at about 12.2 eV, marking the onset of σ-σ transitions in good agreement with the observed growth of the reflectance peak at 14.5 eV. From Fig. 3, we ascribe this peak to the allowed transitions between the highest occupied σ band and the first σ conduction band. The transition energy increases to about 16.3 eV for the Q^+_{2g}-Q^+_{1u} allowed transition, and the flatness of the bands along ΓQ near Q agrees qualitatively with the observed slower decrease in the dielectric function above 15 eV.

For polarization $E \parallel c$, our calculation predicts reflectance structure between about 13.5 and 16.5 eV from the σ-π transitions P^+_3-P^-_3 and Q^+_{1u}-Q^-_{2g}, respectively. Again, since point Q is a saddle point the Q^+_{1u}-Q^-_{2g} transition should contribute strongly to the imaginary part of the dielectric function for $E \parallel c$. This is in qualitative agreement with the observed increase in reflectivity above 10 eV for $E \parallel c$ (Ref. 1). Although there have been energy-loss experiments carried out on graphite to determine the dielectric function of graphite in the direction of the c axis,[18] no reflectivity measurements for $E \parallel c$ have been done above 10 eV.

It does not seem possible, on the basis of this and other band calculations, to adequately explain the structure at 4.8 and 6.0 eV in the lower in-

tensity $E \| c$ reflectivity measurements. Greenaway *et al.*[1] attribute this structure to transitions between the highest σ valence band and the lowest π conduction band, which are forbidden at the points P and Q. The transition Q_{2g}^{+}-Q_{2g}^{-} from our calculation is about 10.3 eV. We should note that the calculated transition L_1-L_1 in the three-dimensional Brillouin zone does occur at 4.6 eV.

There is some question of the propriety of dividing the optical spectra of graphite into regions characterized by π-π and σ-σ electron transitions. Our calculation shows that this separation is justified and that the σ-π valence-band overlap is only 2.6 eV. The occupied σ bands lie about 5.2 eV below the Fermi level. The bandwidths for the σ and π valence bands are given in Table II.

B. Some Results for Multiple-Layer Structure

Including the interaction among layers involves a four atom per unit cell lattice with 12 extra electrons per unit cell. From our calculation, each energy band obtained for the single-layer model slightly splits upon including the interaction among adjacent planes. The spacing between these split almost degenerate bands is less than 0.15 eV over most of the Brillouin zone. However, at certain wave vectors the band splittings are larger and quite important for explaining the electrical properties of graphite. In the single-layer model (Fig. 3), the Fermi energy ($E_F = -0.325$ hartree) passes through the state P_3^- at the point P in the Brillouin zone, characterizing the material as a semiconductor with vanishing energy gap. In the three-dimensional band structure, the states at P_3^- are split, and the energy band dependence on k_z, e.g., along *HPH*, determines the complex Fermi surface and semimetallic properties of graphite. In Fig. 4 are shown the results of our calculation of the energy dependence on k_z along the *HPH* edge of the Brillouin zone, demonstrating the overlap of the π valence and conduction bands. This calculation is in agreement with the results of the Slonczewski-Weiss band model[4,19] in predicting hole occupancy around point P. Recent experimental results[20,21] suggest that the parameters which enter into that scheme have values which imply electron occupancy at P. Further work is planned to correlate our work with the Slonczewski-Weiss model in order to resolve these differences.

TABLE II. Bandwidths of valence bands of graphite.

Band	Width (eV)
π_1	7.35
σ_3	7.07
σ_2	8.43
σ_1	5.90

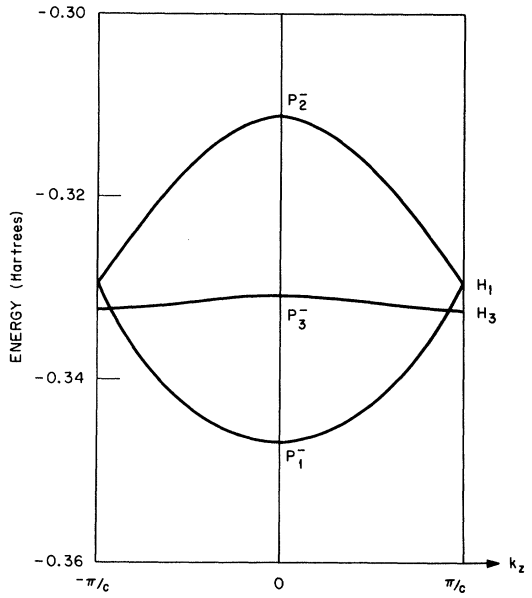

FIG. 4. Energy band dependence upon k_z along the edge *HPH* of the three-dimensional Brillouin zone for multiple-layer graphite lattice. Here the conduction and valence bands overlap so that graphite behaves like a semimetal. The state P_3^- is doubly degenerate.

Other interesting features with regard to the optical properties do appear in the results of the calculation with four atoms per unit cell near the Fermi surface at Q and P. For example, along the directions LQP of the Brillouin zone, the states Q_{2g}^- and Q_{2u}^- each split by about 0.4 eV into Q_{2u}^-, Q_{2g}^-, and Q_{2g}^-, Q_{2u}^-, respectively. From the order of the levels, the energies for the transitions Q_{2u}^--Q_{2g}^-; Q_{2g}^--Q_{2u}^- differ by less than 0.15 eV so that the 4.6-eV peak does not show doublet structure, in agreement with the results of Greenaway *et al.*[1] The point P_3^- in the two-dimensional Brillouin zone is split into states P_2^-, P_3^-, and P_1^- with the P_2^--P_1^- transition at about 0.98 eV. This agrees with the observations of Taft and Philipp[14] of weak reflectance structure near 0.8 eV.

Another interesting feature of the calculation using the four atom per unit cell lattice is a slight depression of the average band structure with regard to the bands obtained with the single-layer crystal. That is, the nearly degenerate bands of the three-dimensional Brillouin zone do not lie equally spaced above and below their two-dimensional analog but are shifted more toward lower energy. This is accentuated at the symmetry point labeled Γ_{2u}^- in the two-dimensional Brillouin zone. In the three-dimensional zone, this state splits into a bonding Γ_{2g}^- and an antibonding Γ_{2u}^- combination of p_z orbitals on adjacent layers with

the bonding state lying about 0.5 eV below the Γ_{2u}^- state in the two-dimensional zone. Computations performed for a single-layer structure, but including the interaction between planes in the crystal potential, indicate that this behavior is due to the formation of a low-energy state rather than the simple inclusion of the potential of the adjacent layers. While the one-electron energies alone are not an adequate basis to quantitatively investigate the total energy, this large splitting behavior at Γ is still of interest with regard to the energy of binding of the graphite layers.

IV. SUMMARY

The *ab initio* variational approach using a Bloch LCAO orbital basis has proven to be quite successful in calculating the band structure and optical transitions for graphite. This is encouraging, considering that an approximate one-electron model Hamiltonian was used, and that there was no parametrization of the matrix elements. Also of interest is the invariance of the band structure with respect to scaling of the exchange potential. The success of the band structure in predicting the optical transition energies for $E \perp c$ leads us to believe that the weak reflectance structure at low energies for $E \parallel c$ may be due to effects other than direct transitions. It would be of interest to extend reflectivity measurements for $E \parallel c$ into the energy range above 12 eV to see if the structure from the transitions $P_3^+ - P_3^-$ and $Q_{1u}^+ - Q_{2g}^-$ is present.

The single-layer structure has been found to be quite adequate for treating the optical transitions in graphite and is an interesting case for further study. It is necessary, however, to consider the multiple-layer lattice in order to properly study the details of the Fermi surface of graphite. Further calculations are in progress to investigate the relation of the band structure in the one-electron approximation to the detailed experimental data on the Fermi surface and electrical properties of graphite.

ACKNOWLEDGMENTS

The authors are grateful to Dr. J. S. Faulkner for encouragement and to Dr. E. T. Arakawa and Dr. R. H. Ritchie for helpful discussions of the results of this work. Computations were performed at the Computation Center at the Oak Ridge National Laboratory.

---

*Research sponsored by the U.S. Atomic Energy Commission under contract with the Union Carbide Corporation, by the Air Force Office of Scientific Research, and by the Advanced Research Projects Agency through the Northwestern University Materials Research Center, Evanston, Ill. 60201.

†Alfred P. Sloan Research Fellow.

[1]D. L. Greenaway, G. Harbeke, F. Bassani, and E. Tosatti, Phys. Rev. 178, 1340 (1969), and references therein.

[2]J. W. McClure, Phys. Rev. 104, 666 (1956).

[3]J. W. McClure, Phys. Rev. 108, 612 (1957).

[4]J. C. Slonczewski and P. R. Weiss, Phys. Rev. 109, 272 (1958).

[5]G. Dresselhaus and M. S. Dresselhaus, Phys. Rev. 140, A401 (1965).

[6]P. R. Wallace, Phys. Rev. 71, 622 (1947).

[7]C. A. Coulson and H. Taylor, Proc. Phys. Soc. (London) A65, 815 (1952).

[8]W. M. Lomer, Proc. Roy. Soc. (London) A227, 330 (1955).

[9]F. J. Corbato, in *Proceedings of the Third Conference on Carbon* (Pergamon, London, 1959), p. 173.

[10]F. Bassani and G. Pastori Parravicini, Nuovo Cimento 50, 95 (1967).

[11]G. S. Painter and D. E. Ellis, Int. J. Quantum Chem. 3S, 801 (1969).

[12]F. Herman and S. Skillman, *Atomic Structure Calculations* (Prentice-Hall, Englewood Cliffs, N.J., 1963).

[13]J. C. Slater, T. M. Wilson, and J. H. Wood, Phys. Rev. 179, 29 (1969).

[14]E. A. Taft and H. R. Philipp, Phys. Rev. 138, A197 (1965).

[15]J. G. Carter, R. H. Huebner, R. N. Hamm, and R. D. Birkhoff, Phys. Rev. 137, A639 (1965).

[16]F. C. Chalklin, Proc. Roy. Soc. (London) A194, 42 (1948).

[17]F. Bassani, *Rendiconti SIF XXXIV Course* (Academic, New York, 1966), p. 33; G. Harbeke, *ibid.*, p. 90.

[18]F. Bassani and E. Tossatti, Phys. Letters 27, 446 (1968).

[19]J. W. McClure, IBM J. Res. Develop. 8, 255 (1964).

[20]P. R. Schroeder, M. S. Dresselhaus, and A. Javan, Phys. Rev. Letters 20, 1292 (1968).

[21]I. L. Spain, in the Third Materials Research Symposium on the Electronic Density of States, Gaithersburg, Maryland, 1969 (unpublished).